H∞ Loop Shaping Based Robust Power System Stabilizer for Dynamic Equivalent Multi-machine Power System

Jayapal R,
Email: rv_rj @ rediff.com

Dr.J K.Mendiratta
Email: mendiratta.jk@gmail.com

Abstract— This paper describes a method of designing H∞ loop shaping based robust power system stabilizer for a coherency based dynamic equivalent large power system. Group of coherent generators are identified on the basis of the equal acceleration. The dynamic equivalent parameters are determined by structure preservation of the coefficient matrices in a time-domain representation of the machines. H∞ loop shaping based robust power system stabilizer is designed for a dynamic equivalent large power system. The method is applied to the well-known IEEE, 10-machine, 39-bus, New England Test System The developed equivalent system has good accuracy in representing the dynamic characteristics of the original system. Results and simulation show that designed H∞ loop shaping based robust power system stabilizer stabilizes the power system very effectively.

Keywords—Coherency Identification, Dynamic equivalent, H∞ loop shaping, Large Power System, power system stabilizer.

I. INTRODUCTION

The size and complexity of modern electric power systems necessitates the construction of reduced-order dynamic models, or dynamic equivalents. Determination of transient stability is one of the major items of power system operation and planning [1].The detailed representation of the machines with their controllers increase in the computational costs of the transient stability studies [2]. The computational effort can be reduced significantly by the exploitation of observed phenomena termed 'coherency'.

It has been observed in multimachine transients that, following a disturbance, some machines swing together, i.e. they have equal velocities and accelerations, and maintain nearly constant angular differences with each other. Such a coherent group of machines can be represented by a single equivalent machine, thereby reducing the number of machines. These reduced order dynamic models for certain parts of the power system are termed coherency-based dynamic equivalents [3].

In the dynamic equivalencing process, the original system is divided into two systems or areas called the 'study system' and 'external system'. The "study system" includes the disturbance and a small number of generators of great concern. These generators are severely disturbed and are generally responsible for the system instability. The rest of the generators are considered in the "external system". The generators in the "external system" do not contribute significantly to the system instability. Thus the dynamic equivalencing technique/methodology is applied to those generators in the "external system" only. Several methods of dynamic equivalencing have been reported in [1]. These can be classified into two categories Modal approach [3], [4] and Coherency approach [2], [5] - [7]. Of these the coherency based approach has received much attention in recent years because of its simplicity and reliability.

This paper uses the Glover-McFarlane H∞ loop shaping design procedure to design the PSS. It combines the H∞ robust stabilization with the classical loop shaping technique. In contrast to the classical loop shaping approach, the loop shaping is done without explicit regard to the nominal plant phase information. The design is both simple and systematic. Some basic guidelines for loop shaping weighting selection and controller design paradigm formulation are also provided.

II. IDENTIFICATION OF COHERENT GENERATORS

Coherency is identified based on equal velocity and acceleration [1]. Coherent groups are identified among those external or remote area machines and each coherent group replaced by a single equivalent machine.

Geographical proximity or electrical proximity [1] for any two machines depends upon their mutual admittance. Mutual admittance between a pair of machines is a measure of coupling between them. Therefore, an electrical proximity index, can be defined by the equation

$$\alpha_{ik} = \frac{(n-1)\left|Y'_{ik}\right|}{\left|Y'_{ii}\right|} \geq 1.0 \quad \text{for } k = 1, 2, 3\ldots n \text{ and for } k \neq i \qquad (1)$$

The dummy variable Y'_{ij} is related to the actual system admittance matrix element Y_{ij} as follows

$$Y'_{ij} = Y_{ij} \quad \text{a} \quad Y'_{ii} = -\sum_{\substack{j=1 \\ j \neq i}}^{n} Y_{ij} \qquad (2)$$

Where $\left|Y_{ij}\right| \angle \theta_{ij}$ is the transfer admittance between the 'i^{th}' and 'j^{th}' generator nodes in the reduced network. The reduced network is obtained by eliminating all the terminal buses and load buses of the network retaining the internal generator nodes only [10]. Only such generators whish satisfy (1) are considered for coherency grouping test with the i^{th} machine.

Two normalized indices [1], [4] β and γ, which taken together will give an estimate of the coherency between the generators i and j

.The β and γ defined as $\beta_{ij} = \frac{|M_i - M_j|}{Max(M_i, M_j)}$ (3)

$$\gamma_{ij} = \frac{|M_i^{-1}D_i - M_j^{-1}D_j|}{Max(M_i^{-1}D_i, M_j^{-1}D_j)_{ji}} \quad (4)$$

For perfect coherency, both β_{ij} and γ_{ij} must be identically equal to zero. This condition is rarely satisfied in practical systems. If one of the inertias tends to infinity both β_{ij} and γ_{ij} will tend to 1 indicating generators are deviating from each other. However in practice, $\beta_{ij} \leq 0.5$ and $\gamma_{ji} \leq 0.5$ are considered [1] to be satisfactory to conclude that the machines are coherent. If damping is considered uniform for all the machines, i.e. *Di/Mi = Dj/Mj,* or neglected, then the coherency between *ith* and *jth* generators will depend on the value of β_{ij} alone. If *Mi = Mj*, then the coherency between i^{th} and j^{th} generators will depend on the value of γ_{ij} alone.

The method of coherency identification is tested by application to IEEE, 10-machine, 39-bus, New England Test System [12]. A 3-phase to ground fault in the line connecting buses 26 and 29(automatic clearing) is considered. The power is calculated during the fault and after the fault is cleared at all the generators. The generators which exceed the variation in power by more than 30% are considered to be in study system and the rest are considered as external system. For the example considered Generators 2, 8 and 9 are in the study system.

A generalised program is developed in MATLAB to implement the procedure highlighted. The output of the program is displayed in the Tables- (I &II) which show the values of α, β and γ indices.

TABLE-I. α – INDEX

M/c NO.	1	2	3	4	5	6	7	8	9	10
1	1.00	2.07	3.79	0.23	0.53	0.56	0.31	0.49	0.19	0.85
2	2.01	1.00	1.59	0.17	0.39	0.41	0.22	1.34	0.28	2.63
3	3.60	1.55	1.00	0.31	0.71	0.75	0.41	0.54	0.23	0.91
4	0.24	0.18	0.34	1.00	6.29	0.81	0.44	0.24	0.16	0.32
5	0.40	0.30	0.56	4.54	1.00	1.32	0.72	0.39	0.26	0.53
6	0.46	0.34	0.64	0.63	1.43	1.00	4.17	0.45	0.29	0.61
7	0.33	0.25	0.47	0.45	1.03	5.52	1.00	0.32	0.21	0.44
8	0.47	1.34	0.55	0.22	0.50	0.53	0.29	1.00	0.97	4.20
9	0.48	0.73	0.60	0.38	0.87	0.92	0.50	2.55	1.00	2.00
10	0.65	2.09	0.74	0.24	0.54	0.58	0.31	3.33	0.60	1.00

TABLE-II. β and γ- INDICES

M/c NO.	1	2	3	4	5	6	7	8	9
2	0.94								
3	0.15	0.93							
4	0.14	0.95	0.27						
5	0.06	0.94	0.20	0.09					
6	0.13	0.93	0.03	0.25	0.18				
7	0.13	0.95	0.26	0.02	0.08	0.24			
8	0.20	0.95	0.32	0.07	0.15	0.30	0.08		
9	0.12	0.93	0.04	0.25	0.17	0.01	0.23	0.30	
10	0.28	0.92	0.15	0.38	0.32	0.17	0.37	0.42	0.18

For the example considered damping coefficient, D=0. Hence β and γ indices are the same. By checking α, β and γ values of the machines in the remote area, the following coherent groups are identified.

Group-I Machine Number 1 and 3

Group-II Machine Number 4, 5, 6 and 7

To justify the above results the model of the example considered is created using simulink available in MATLAB, using the differential and algebraic equations applicable for model 1.1[12]. The simulation results are shown in Fig 1and Fig 2. Fig1 shows the plot of rotor angles of coherent group1 for m/c1 and m/c3 while Fig2 shows the plot of rotor angles of coherent group2 for m/c4,m/c5.m/c6 and m/c7. From the above results it is justified that the method of identification of coherent groups is accurate.

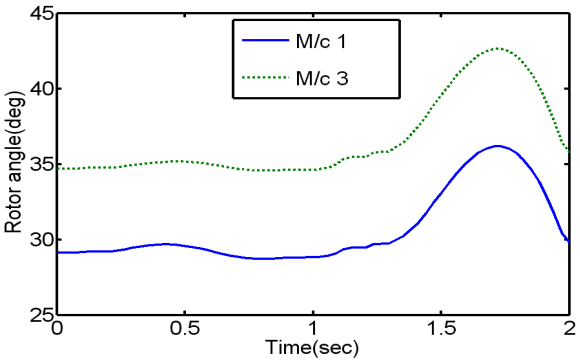

Fig.1. Plot of rotor angle at M/c1 and M/c3..

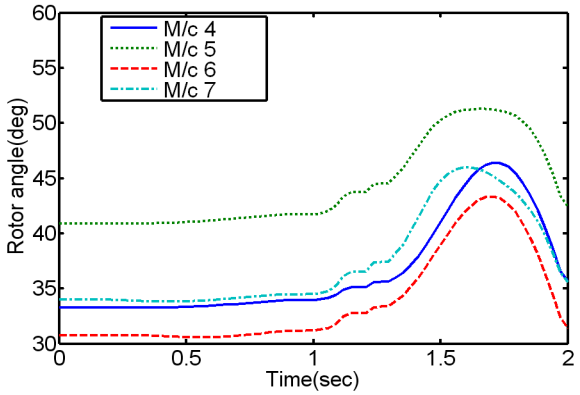

Fig.2. Plot of rotor angle at M/c4, M/c5, M/c6 and M/c7.

III. CONSTRUCTION OF DYNAMIC EQUIVALENT

Several approaches have appeared in the literature [6]-[9] to represent a coherent group of machines by an equivalent machine. However, most of these approaches deal with equivalencing of machines represented by classical models while in this paper the dynamic aggregation is applied to model 1.1[12]. A method for constructing dynamic equivalents is based on coherency, i.e. the generators whose transient behavior is similar to each other are aggregated into an equivalent generator. This method [6] does not require any iteration to determine the parameters of the equivalent synchronous machine and equivalent excitation system. It should be noted that the various coefficient matrices in time-domain representation of the power system components have a pattern of zero, non-zero entries known as the prespecified structure of coefficient matrices. Thus, the reduced order dynamic equivalents retain the characteristics of normal system and hence can be used with the standard transient stability programs without any modification.

A. Shaft dynamics model [6]:The swing equation representing the shaft dynamics of an individual machine is

$$2H\dot{\omega} = P_m - P_g - D\omega \quad (5)$$

As all machines have the same speed deviation ω, eqn. 16 can be summed for m coherent machines to yield

$$(\Sigma 2H)\dot{\omega} = \Sigma P_m - \Sigma P_g - (\Sigma D)\omega \quad (6)$$

Eqn. 5 is similar to eqn. 6 and can be used to represent the shaft dynamics of the equivalent model if

$$H^* = \Sigma H,\ P^*_G = \Sigma P_g,\ P^*_M = \Sigma P_m \text{ and } D^* = \Sigma D \quad (7)$$

Where superscript *- stands for the corresponding parameters of the equivalent machine.

B. Synchronous machine model: It is assumed that the individual machines are represented by a two-axis model with one field winding in the direct axis and one damper winding in the quadrature axis. For such a representation, using the structure preserving technique [6], the equivalent machine synchronous reactances X^*_D and X^*_Q, the transient reactances of the equivalent machine X'^*_D and X'^*_Q and the transient open circuit time constants T'^*_{qo} and T'^*_{do} are obtained without any iteration. These parameters are used in the standard representation of a 2-axis model.

C. Excitation system model: In reference [6], it is assumed that the individual machines are represented by third order IEEE type 1 excitation system. But for the example considered in this paper, the excitation system is of first order and more over same excitation is used at all the machines. Hence there is no necessity for dynamic aggregation. Excitation system with K_A=25 and T_A=0.025 is used at all machines.

The two coherent groups identified in the earlier section are replaced by the corresponding equivalent machines using the above method of constructing dynamic equivalent and the equivalent parameters along with original values are as shown in the Table III and Table IV.

TABLE-III. ORIGINAL AND DYNAMIC EQUIVALENT PARAMETERS OF GROUP I

M/c No.	x_d	x_q	x'_d	x'_q	T'_{do}	T'_{qo}	H
1	0.2950	0.2820	0.0647	0.0647	6.56	1.5	30.3
3	0.2495	0.2370	0.0531	0.0531	5.70	1.5	35.8
Equi-valent	**0.1288**	**0.1352**	**0.0292**	**0.0292**	**5.9875**	**1.5012**	**66.1**

TABLE-IV. ORIGINAL AND DYNAMIC EQUIVALENT PARAMETERS OFGROUP II

M/c No.	x_d	x_q	x'_d	x'_q	T'_{do}	T'_{qo}	H
4	0.3300	0.3100	0.0660	0.0660	5.4	0.44	26.0
5	0.2620	0.2580	0.0436	0.0436	5.69	1.5	28.6
6	0.2540	0.2410	0.0500	0.0500	7.3	0.4	34.8
7	0.2950	0.2920	0.0490	0.0490	5.66	1.5	26.4
Equi-valent	**0.0681**	**0.0705**	**0.0127**	**0.0127**	**5.5487**	**1.0644**	**115.8**

Once the parameters of the dynamic equivalent machines are determined, generators 1 and 3 are replaced by a single dynamic equivalent generator. Similarly generators 4, 5, 6 and 7 are replaced by another single dynamic equivalent generator. Hence the 10-M/c, 39 bus system is reduced to 6-M/c, 35 bus system.

Simulation is performed for 2 seconds on original system as well as on the equivalent system for a three phase to ground fault on the line considered earlier for coherency identification and some of the results are shown in Fig 3 and Fig 4. From these, it can be observed that the performance of the dynamic equivalent system matches with the performance of the original system, with allowable deviation.

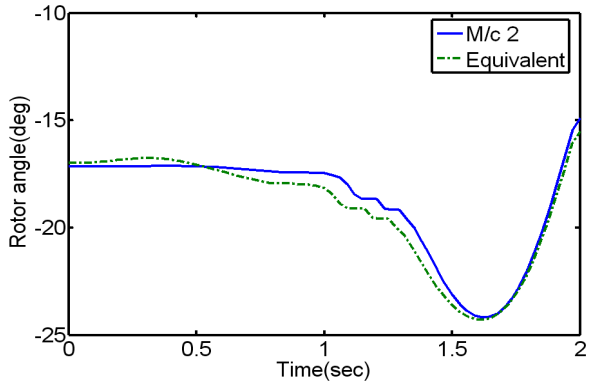

Fig3. Rotor angle plot of M/c 2 and its equivalent.

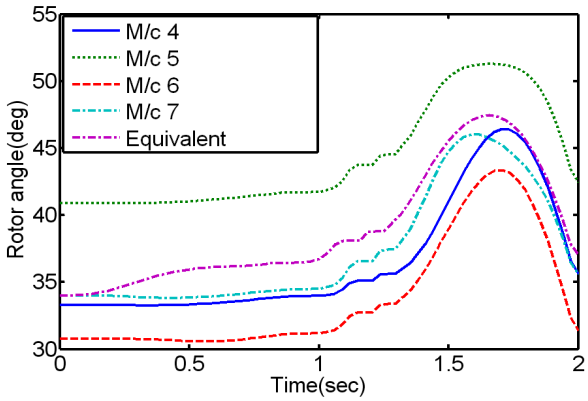

Fig4.Rotor angle plot of M/c 4, M/c 5, M/c 6, M/c 7 and their equivalent

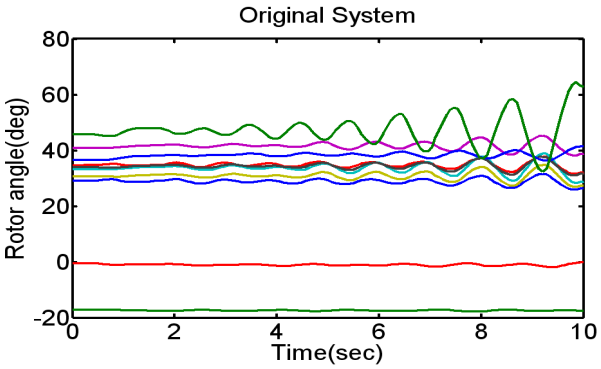

Fig5.Rotor angle at all the machines of original system

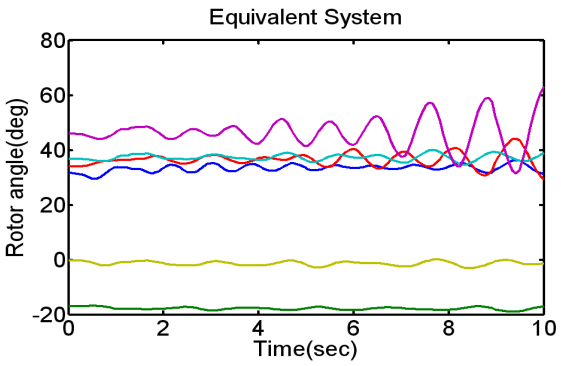

Fig6.Rotor angle at all the machines of equivalent system

The steady state response of the original and the dynamic equivalent systems are simulated. The steady state response of the

original system is shown in Fig 5 and that of the equivalent system is shown in Fig6.From these two plots it can be observed that the steady state responses of the equivalent system matches with the original system.

IV. DESIGN OF ROBUST POWER SYSTEM STABILIZER.

Glover-McFarlane H∞ loop shaping technique is employed to design a robust power system stabilizer for the dynamic equivalent six machine system. The procedure is highlighted as under:

A. Robust controller design: The Glover-McFarlane H∞ loop shaping design procedure [11], [15],[17] consists of three steps:

1. Loop shaping:
2. Robust Stabilization
3. The final feedback controller K

B. Loop Shaping: This procedure is applied to the example considered. The state matrix representation of the original 10-M/c, 39 bus system is obtained. The Eigen values of this system correspond to the inter-area mode. The damping ratio of the system is computed. The system has poor damping at frequency 3.71 and 5.68 rad/sec.The objective of loop shaping is to increase the open-loop gain around these frequencies [15].

C. Selection of W_1: We add pole and zero pairs to achieve gain increase in the desired frequency range while keeping the gain change as small as possible around other frequency values [11]. A washout filter block in W_1 with time constant 10s is used to ensure the controller only works in the transient state [15]. The selection of the pole at 1/0.2695 and the zero at 1/0.33 increased the gain around the frequencies of interest so that the plant input disturbance can be attenuated effectively. The resulting transfer function for the weighting

$$W_1 = \frac{10^4 * 10s * (1+0.33s)}{(1+10s)(1+0.2695s)(1+0.1761)} \quad (9)$$

D. Selection of W_2: With W_2=1, the open loop gain Gs=W_2GW_1 was very less and more over the slope of the shaped plant was low at low frequencies. To increase the gain of the system at low frequency, three repeated zeros are added at frequency 10. To make W_2 proper and to achieve proper slope of Gs at cross over frequency three poles are added at insignificant frequency of 300. The reduced dc gain of W_2 is compensated by using a constant 1000 [15]. The resulting transfer functions for the weighting

$$W_2 = \frac{10^3 * (s+10)^3}{(s+300)^3} \quad (10)$$

The resulting singular value plot of nominal system G, W1, W2 and Gs are shown in Fig 7.

E. H∞ synthesis: Next, we synthesized a K∞ controller to achieve robust stability for the nominal plant. The maximum stability margin is $\varepsilon_{max=}$ 0.2473. This margin evaluates the feasibility of our loop shaping design. According to McFarlane and Glover [11], given the normalized left coprime factorization of the nominal plant as $Gs_0 = \overline{M}_s^{-1}\overline{N}_s$, the controller K∞ can stabilize all Gs = $(\overline{M}+\Delta_M)^{-1}(\overline{N}+\Delta_N)$ satisfying $\|\Delta_M, \Delta_N\|_\infty < 0.2473$. Furthermore, this controller stabilizes a gap ball of uncertainty with a given radius if and only if it stabilizes a normalized coprime factor perturbation ball of the same radius. Thus, in terms of the gap metric, all Gs with $\delta_g(Gs,Gs_0) < 0.2473$ can be stabilized by this controller.

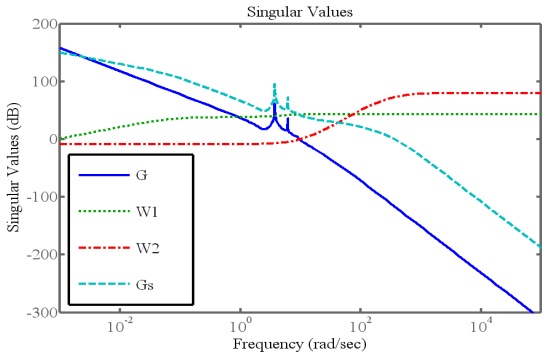

Fig7. The singular value plot of G, W1, W2 and Gs

F. The final controller K: The final controller is the combination of $W_1$and W_2 with K∞, that is K=W_1 K∞ W_2. This gives 10 controllers from 10 inputs to the output such as K (1, 1), K (1, 2)….K (1, 10). To find the best of the 10 controllers Bode magnitude plot of each controller is compared with the Bode magnitude plot of general controller K.The controller whose Bode magnitude plot closely matches with the Bode magnitude plot of general controller is selected as the best controller. For the example considered K (1, 9) matches with the general controller K as shown in Fig8.

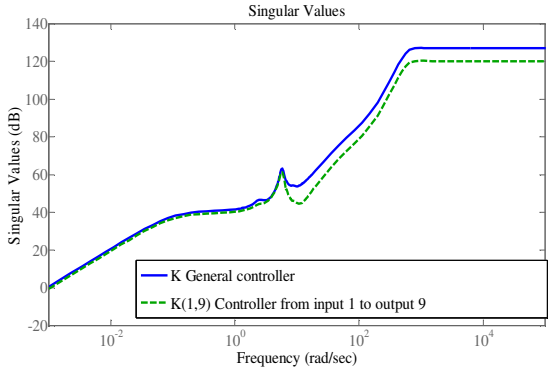

Fig8. The singular value plot K and K (1, 9)

G. Controller order reduction: We want to conduct a nonlinear simulation using simulink to examine the performance of the designed controller. The resulting controller has a high order. The controller is reduced to a 7th order controller using the Hankel Norm reduction [14]. The transfer function of the reduced order controller is given as Gk(s) =N(s)/D(s), with

N(s) = $2.46*10^6 s^7 + 2.542*10^9 s^6 + 9.494*10^{11} s^5 + 1.452*10^{14} s^4 + 7.403*10^{15} s^3 + 1.312*10^{17} s^2 + 9.426*10^{17} s + 1.146*10^{16}$

D(s) = $s^7 + 2541 s^6 + 3.205*10^6 s^5 + 2.349*10^9 s^4 + 9.754*10^{11} s^3 + 2.047*10^{14} s^2 + 1.678*10^{16} s + 9.807*10^{14}$

The bode plots of the full-order controller and the reduced-controller are shown in Fig. 9. This final controller is used at all the necessary machines depending upon the participation factors of various swing modes as explained later. Since the common controller is used at all the necessary machines, the dynamic aggregation does not alter the controller transfer function. Hence the controller used for the original system is used for the equivalent system as well.

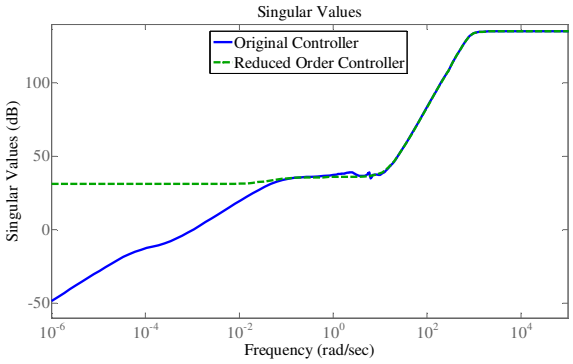

Fig9. Bode plot of the actual and reduced order controller

If the PSS design is based on the one machine infinite bus model , after the installations of PSSs on most machines of a large power system, low frequency oscillations may still occur due to lack of coordination of these stabilizers[16]. Hence coordinated application of PSSs is required. To achieve the coordination, the state matrix of the entire system is used to design PSS using Glover-McFarlane H∞ loop shaping design procedure. Using participation factor technique [13], [18], the selected stabilizers are placed only at the machines where PSS is most essential. For the example considered, the Eigen values associated with the four swing modes at the given operating point without PSS are given in Table V. Table VI gives the participation factors (magnitude) of the system in modes M1 toM4. The speed of that machine with highest participation in a particular mode is the best signal to damp the oscillations due to that mode. In Table VI, Smi correspond to slip of i^{th} machine.

TABLE IV. EIGEN VALUES OF THE SYSTEM

Swing mode	Without PSS
M1	-0.52867 ± 7.3812i
M2	-0.070722 ± 6.6112i
M3	0.29545 ±5.6989i
M4	0.0094119 ± 3.8554i

TABLE V. PARTICIPATION FACTORS(*-INDICATES SMALL VALUES)

Mode	*Sm1*	Sm2	Sm3	Sm4	Sm5	Sm6
M1	0.026	*	0.025	**0.425**	0.036	0.108
M2	**0.420**	0.023*	0.047	*	.*	*
M3	*	**0.180**	0.150	*	**0.317**	*
M4	*		0.175	0.027	0.090	0.031

Hence it can be observed from Table VI that generator4, generator1 and generator5 control the swing modes M1, M2 and M3 respectively while generator2 control the swing mode M4. This mode (M4) is insignificant as the corresponding participation factor is comparatively small. Hence generator1, generator4 and generator5 are the best locations to place PSSs to damp modes M1 to M4.

Comparison of RPSS with CPSS: Next nonlinear simulations are performed with Robust PSS (RPSS) and conventional PSS (CPSS) (Refer Appendix), at the necessary machines. A Three Phase to ground fault is created at a line connected between the buses 26 and 29 near bus no29. The fault is initiated after 1 second and automatically cleared at the end of 5cycles. Fig 10 shows the plots of rotor angles of all equivalent machines with respect to COI, during fault with RPSS, while Fig11 shows the same plots with CPSS. From these plots it can be observed that the system becomes stable within 5 seconds with RPSS, while the system takes more time to reach stability with CPSS.

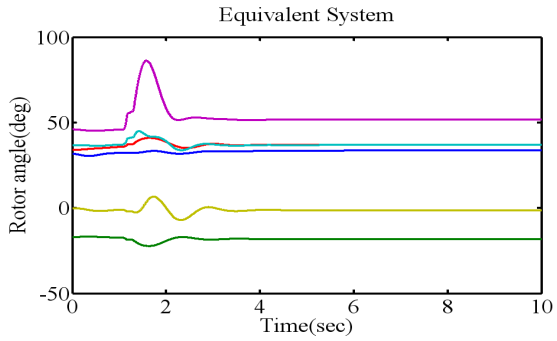

Fig10.Plot of rotor angles at all equivalent machines with RPSS with a 3 phase fault

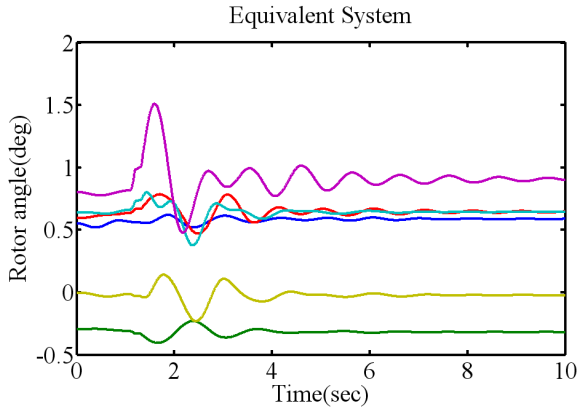

Fig11.Plot of rotor angles at all equivalent machines with CPSS with a 3 phase fault

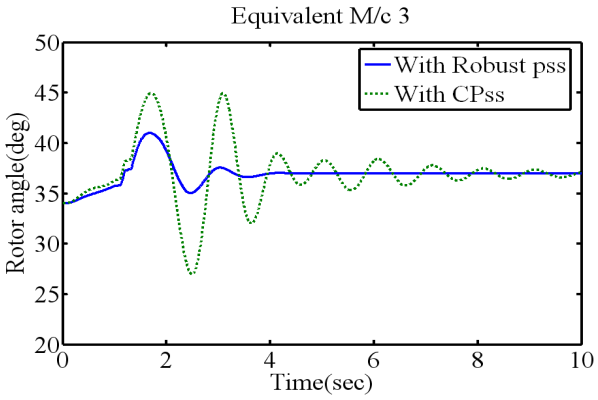

Fig12.Plot of rotor angle at equivalent machine 3, with RPSS and CPSS with a 3 phase fault.

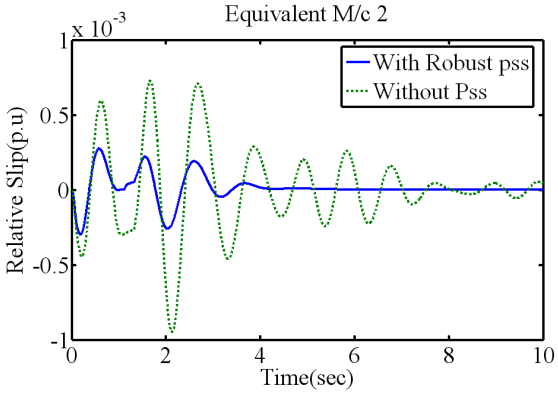

Fig13.Plot of relative slip at equivalent machine 2, with RPSS and CPSS with a 3 phase fault.

The simulation is performed under three phase fault condition and comparisons of rotor angles, slip and electric torque are plotted at all the machines and some of the results are shown from Fig 12 to Fig14.From these, it can be observed that the transients in the system with RPSS vanish faster compared to system with C PSS and reaches steady state within 4 to 5 seconds consistently, justifying robustness. In case of system with CPSS transients exists for a longer duration and system reaches steady state very slowly and the settling time is inconsistent.

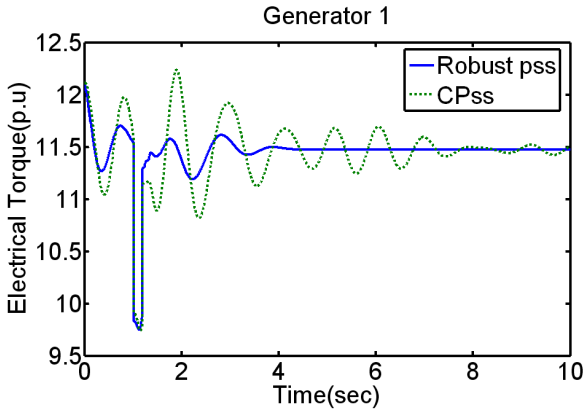

Fig14.Plot electrical torque at equivalent machine 1 with RPSS and CPSS with a 3 phase fault

V. CONCLUSION

This paper has described a procedure for coherency identification technique based on equal acceleration concepts, dynamic equivalent based on structure preserving technique and design of a robust power system stabilizer based on Glover-McFarlane H∞ loop shaping technique. The procedure is illustrated on the New England Test System. The original 10-M/c, 39 bus system is reduced to dynamic equivalent of 6-M/c, 35 bus system. Simulations are performed to assess the accuracy of the equivalent model by comparing with the original system. Results of the simulation show that the developed equivalent system has good accuracy in representing the dynamic characteristics of the original system.

A RPSS based on Glover-McFarlane H∞ loop shaping technique is designed for the system considered. The performance of the designed RPSS is compared with CPSS. The simulation results show that the RPSS is more effective in damping the transients compared to CPSS.

This method can easily be extended to a very large power system, which can be represented by reduced equivalent system, for which a RPSS can be designed to control the entire system effectively.

VI. REFERENCES

[1] Gurupradada Rau, V. and Yeakub Hussain, Md. 'Coherent Generators' © 1998, Allied Publishers Limited.

[2] Van Orisouw, P.M., 'Dynamic Equivalent Using Modal Coherency and frequency response', IEEE Trans., Vol. Ps-50, N0.1, Feb 1990, pp.289-95.

[3] Spadling, B.D., Yee,H. and Goudie,D.B., 'Coherency Recognition for Transient Stability Studies Using Singular Points, IEEE Trans., Vol. PAS-96, 1977, pp.1368-1375.

[4] Yeakub Hussain, Md and Gurupradada Rau, V., 'A Faster Method of Coherency Identification and System Equivalents and Transient Stability Studies', Proceeding of the 13th National Systems Conference, December 13-15, System Society of India, 1989,pp323-26.

[5] Hiyama,T., 'Identification of Coherent Generators Using Frequency Response, Proceedings of the IEE, Vol. 128,pt C, No.5, September 1981,pp.262-68.

[6] R. Nath. B.Sc.(Eng.), Ph.D.. and Prof. S.S. Lamba, M.Tech., Ph.D.'Development of coherency-based time-domain equivalent model using structure constraints', *Iee Proceedings, Vol. 133, Pt. C, No. 4, May 1986*

[7] Podmore, R. 'A Comprehensive Program for Computing Coherency Based Dynamic Equivalents', IEEE, Power Industry Computer Application Conference, 1979.

[8] Van Orisouw, P.M., Dynamic Equivalent Using Modal Coherency and frequency response', IEEE Trans., Vol. Ps-50, N0.1, Feb 1990, pp.289-95.

[9] Chang, A. and Adibi, M.M., 'Power System Dynamic Equivalent', IEEE Trans., Vol. PAS-89, 1970, pp.1737-44

[10] Anderson, P.M and Foud, A.A., 'Power System Control and Stability', Vol.1 The Iowa State University Press Ames, Iowa, USA, 1977

[11] D.C. MacFarlane and K. Glover, '*A loop shaping design procedure using H∞ synthesis'*, AC-37: 759–769, 1992

[12] Padiyar K.R., '*power system Dynamics stability and control'*, second edition, BS publications, 2002.

[13] P. Kundur, '*Power System Stability and Control'*, New York: McGraw-Hill, 1993.

[14] Matlab Help Documentation Release 12.

[15] Chuanjiang Zhu, *Member, IEEE*, Mustafa Khammash, *Senior Member, IEEE*, Vijay Vittal, *Fellow, IEEE*, and Wenzheng Qiu, *Student Member, IEEE,'* Robust Power System Stabilizer Design Using Loop Shaping Approach', IEEE Transactions On Power Systems, Vol. 18, No. 2, May 2003.

[16] Yao-nan Yu, 'Electric Power system Dynamics', Academic Press 1983.

[17] Jayapal.R and Dr.J.K.Mendiratta, 'Robust power system stabilizer design using H∞ loop shaping approach for single machine system', International conference, CPRI, Bangalore, ICPS 2005.

[18] K.R. Padiyar and H.V. Saikumar, 'Modal Inertia — A New Concept for the Location of PSS in Multimachine Systems', National Systems Conference, Nsc2003.

VII. APPENDIX

The schematic representation of Conventional Power System Stabilizer (CPSS) is as shown in the Fig. 15.

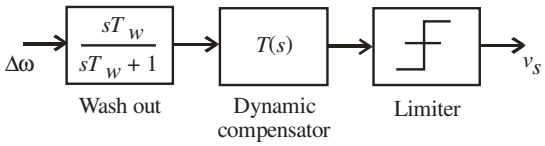

Fig. 15: Conventional Power system Stabilizer

In the block diagram of the CPSS shown, the transfer function $T(s)$ is finally obtained as

$$T(s) = \frac{Ks(1+sT_1)(1+sT_3)}{(1+sT_2)(1+sT_4)}. \qquad (11)$$

The designed parameters of CPSS for the system considered are taken as

$K_S = 15,\ T_1 = 0.75\,s,\ T_2 = 0.3\,s,\ T_W = 10, T_3 = 0$ *and* $T_4 = 0$.

Limits on V_s as $+0.05$ & -0.05.